Optimum Design of a Pin-Fins Type Heat Sink Using the CFD and Mathematical Optimization

Kyoungwoo Park†, Park-Kyoun Oh, Hyo-Jae Lim

Department of Mechanical Engineering, Hoseo University, Asan, Chungnam 336-795, Korea

Key words: Optimum design, Pin-fins heat sink, CFD, Unconstrained optimization, BFGS method

ABSTRACT: The shape of 7×7 pin-fins heat sink is optimized numerically to obtain the minimum pressure drop and thermal resistance. In this study, the fin height (h), fin width (w), and fan-to-heat sink distance (c) are chosen as the design variables and the pressure drop (ΔP) and thermal resistance (θ_j) are adopted as the objective functions. To obtain the optimum design values, we used the finite volume method for calculating the objective functions, the BFGS method for solving the unconstrained non-linear optimization problem, and the weighting method for predicting the multi-objective problem. The results show that the optimum design variables for the weighting coefficient of 0.5 are as follows: w=4.653 mm, h= 59.215 mm, and c=2.667 mm. The objective functions corresponding to the optimal design are calculated as ΔP=6.82 Pa and θ_j=0.56 K/W. The Pareto solutions are also presented for various weighting coefficients and they will offer very useful data to design the pin-fins heat sink.

Nomenclature

c	: fan-to-heat sink distance [m]
c_P	: specific heat [J/kg·K]
C_1, C_2, C_3, C_μ	: empirical constants in the k-ε model
$F(\boldsymbol{X})$	: objective function
G_b, G_k	: generation terms in the k-ε eqs.
g_i	: acceleration of gravity [m/s^2]
h	: fin height [m]
H	: height of heat sink($=h+t$) [m]
$\boldsymbol{H}$	: Hessian matrix
k	: turbulent kinetic energy [m^2/s^2]
k_s	: thermal conductivity for solid [W/m·K]
l	: characteristic length [m]
L	: length and width of heat sink [m]
P	: pressure [Pa]
ΔP	: pressure drop [Pa]
Q	: dissipated heat [W]
s	: fin spacing [m]
$\boldsymbol{S}$	: search direction in Eq. (15)
t	: basement thickness [m]
T	: temperature [K]
u, v, w	: velocities in x-, y-, z-direction [m/s]
u_i, u_i'	: average and fluctuating velocity [m/s]
w	: fin width [m]
$\boldsymbol{X}$	: design variable vector
x_i	: Cartesian coordinates [m]

Greek symbols

α	: step length parameter in Eq. (15)

† Corresponding author
Tel.: +82-41-540-5804; fax: +82-41-540-5808
E-mail address: kpark@office.hoseo.ac.kr

α_t : eddy diffusivity for heat [m^2/s]
β : thermal expansion coefficient [1/K]
δ, γ : change vectors, in Eq. (18)
δ_{ij} : Kronecker delta
ε : dissipation rate of k [m^2/s^3]
θ_j : thermal resistance [K/W], in Eq. (21)
μ_t : eddy viscosity [$N \cdot s/m^2$]
ρ : density [kg/m^3]
$\sigma_k, \sigma_\varepsilon$: turbulent Prandtl, Schmidt numbers
ϕ : general dependent variable
ω_i : weighting coefficients for pressure drop and thermal resistance, respectively

Subscripts

in : inlet
j : junction
k : number of iterartion
∞ : ambient

1. Introduction

Recent trends for higher power density and smaller package size in electronic systems demand more effective cooling mechanisms for reliability of the electronic device. The forced air cooling technique for heat sinks has been commonly used in a conventional size of heat sink. In addition, the size of heat sinks is determined according to the limited space they are to be installed in. Therefore, they must be designed by considering the pressure drop and the available space as well as the thermal performance. For this reason, the importance of numerical optimization in the design of heat exchangers has been gradually emphasized.

In recent years, many algorithms for numerical optimization technologies have been proposed in order to offer a logical approach to design automation. In addition, as the physical phenomena considered in industrial applications become more complicated, the use of commercial CFD (computational fluid dynamics) codes is dramatically increased. Therefore, the combined field of computational flow/thermal optimization (CFTO) has been receiving much attention. The study of Gallman et al.,[1] however, was mainly restricted to the aircraft design and dealt mostly with aerodynamic shape optimization. A more recent study showed that the technique of combination of CFD and CAO (computer aided optimization) was applied to other fields by Craig et al.[2] In practical situations, it is very difficult to combine commercial CFD solvers with mathematical optimization methods because all of the commercial CFD codes solve the flow and thermal characteristics on the GUI (graphical user interface). Recently, Park et al.[3] studied the design optimization of the plate-fin and tube heat exchanger. They integrated FLUENT, which is a commercial CFD code, and the optimization technology and then proposed the optimum design variables of a heat exchanger.

Augmentation of the thermal performance of heat sink has been receiving considerable attention for many years because of its importance over a wide range of industrial applications. Even though the significant improvement in thermal performance of heat sink has been acquired by using the micro channel heat sink, it is true that the conventional or mini-sized heat sink is still commonly used in many industrial applications as cooling devices.

Much research on the optimization of heat sink has been conducted. However, most of them have focused on the parametric study which influences the flow and thermal characteristics for obtaining the optimum design. Ledezma et al.[4] studied the optimal spacingon a pin-finned plate exposed to an impinging air stream. They used the commercial CFD solver (FIDAP) to solve the flow fields and proposed the correlations for optimal spacing and maximum thermal conductance. The optimal spacing of the nozzle-to-heat sink in impinging air flow

was obtained by Maveety and Hendricks.[5] They concluded that the optimal performance is achieved when the nozzle is placed within the dimensionless vertical distance of eight to twelve from the heat sink ($8 \leq z/D \leq 12$). Recently, Wirtz and Zcheng[6] have described a methodology for determining an optimum fin configuration for the fan-driven heat sink.

Although the aforementioned researches can be useful in designing a heat sink, they just proposed the correlation equations for the optimum design variables by considering only the flow and thermal characteristics of heat sink. It means that the previous works carried out optimization without considering the mathematical optimization technique. Therefore, in this study, in order to obtain the optimal values of the design variables of pin-fins heat sink, we combined the CFD and CAO using the developed scripter file for the batch-job in optimization process. the weighting coefficient effect on the optimal solutions is investigated.

2. Theoretical analysis

2.1 Heat sink with pin-fins

The optimization problem considered in this study is to maximize the thermal performance of the fan-driven heat sink with 7×7 array of pin-fins. Figure 1 depicts the physical configuration of the square pin-fins heat sink schematically. It is made of aluminum and is fabricated by extruding technique. The overall dimensions of heat sink are a length and width of L=65 mm and a height of H=65 mm. Noting that the height of the heat sink (H) is the sum of the fin height (h) and base thickness of heat sink (t). Figure 1 also shows the detailed dimensions of the heat sink and it is a quarter of the full domain of the heat sink. An axial fan, which is apart from the heat sink with some distances (c), impinges cooling air normal to the fin array with the fan-induced swirl, and then the impinged air exits in the x- and y-direction through flow passages between fins. A silicon chip with dimensions of 12×12 mm in the center of the bottom wall uniformly

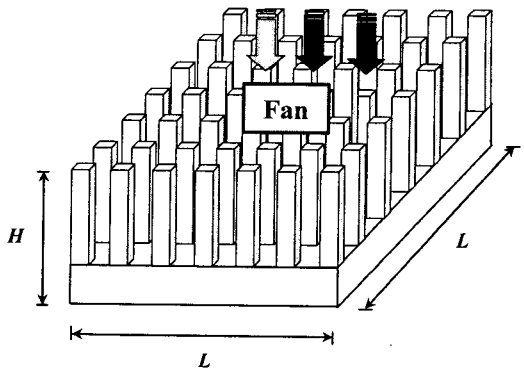

Overview

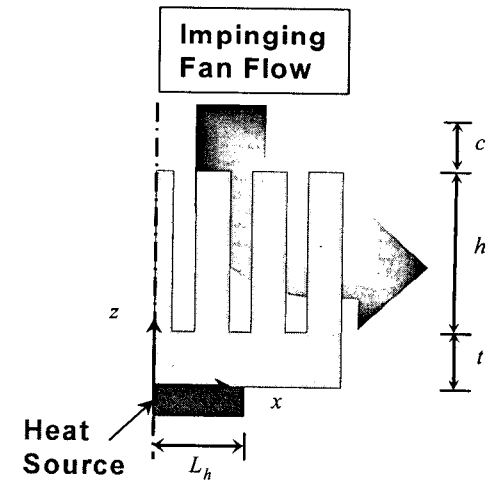

Front-view for computational domain

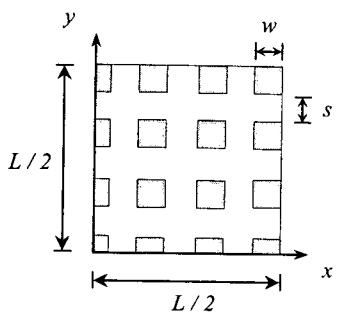

Top-view for computational domain

Fig. 1 Schematics of pin-fins heat sink.

generates the heat by an electric resistance heater (40 W). The heat generated in the heat source is transferred through the pin and fins by conduction at first and then it is rejected from the heat sink to the environment by means of forced convection at the fin-air interfaces. Thus, the problem considered becomes a conjugated heat transfer problem.

2.2 Flow and thermal fields

2.2.1 Governing equations

The fluid properties are assumed constant except for the density in the buoyancy terms of the momentum equation. The flow is considered to be steady, incompressible, and turbulent. The effects of viscous dissipation and radiation heat transfer are assumed to be negligibly small. Due to the symmetric geometry, the computation is only carried out on a quarter of the physical domain. Using assumptions, the time averaged governing equations for mass, momentum, and energy can be expressed in Cartesian tensor form as follows:

Continuum

$$\frac{\partial}{\partial x_j}(\rho u_j) = 0 \tag{1}$$

Momentum

$$\frac{\partial}{\partial x_j}(\rho u_i u_j) = -\frac{\partial P}{\partial x_i} + \frac{\partial}{\partial x_j}\left(\mu \frac{\partial u_i}{\partial x_j} - \overline{\rho u_i' u_j'}\right) + \rho g_i \tag{2}$$

Energy

$$\text{Fluid}: \quad \frac{\partial(\rho u_j T)}{\partial x_j} = \frac{\partial}{\partial x_j}\left(\Gamma \frac{\partial T}{\partial x_j} - \overline{\rho u_i' t'}\right) \tag{3}$$

$$\text{Solid}: \quad \frac{\partial}{\partial x_i}\left(k_s \frac{\partial T}{\partial x_i}\right) + \dot{q} = 0 \tag{4}$$

where i=1, 2 and 3 denote x, y, and z-directions, respectively. $\dot{q}$ is the rate of heat generation per unit volume in the conduction equation of Eq. (4).

In Eqs. (2) and (3), the Reynolds stress, $\overline{\rho u_i' u_j'}$, and the turbulent heat flux, $\overline{\rho u_i' t'}$, which govern the turbulent diffusion, should be determined. Using the eddy viscosity concept, they are defined as follows

$$\overline{\rho u_i' u_j'} = -\mu_t\left(\frac{\partial u_i}{\partial x_j} + \frac{\partial u_j}{\partial x_i}\right) + \frac{2}{3}\rho k \delta_{ij} \tag{5}$$

$$\overline{\rho u_i' t'} = \alpha_t \frac{\partial T}{\partial x_i} \tag{6}$$

where μ_t and α_t are the turbulent (or eddy) viscosity and the eddy diffusivity for heat, respectively. They are computed as

$$\mu_t = \rho C_\mu \frac{k^2}{\varepsilon} \tag{7a}$$

$$\alpha_t = C_\lambda f_\lambda k\left(\frac{k}{\varepsilon}\right)^n \left(\frac{\overline{t'^2}}{\varepsilon_t}\right)^m \tag{7b}$$

where C_λ, f_λ denote the model constant and function including the near wall effect in a thermal field. To obtain the eddy viscosity and eddy diffusivity, the closure problem of the governing equations has to be resolved. Thus, the standard k-ε turbulence model[7] is introduced in this work. According to the eddy-viscosity concept, the turbulent kinetic energy (k) and its dissipation rate (ε) are obtained from the following transport equations:

$$\frac{\partial}{\partial x_j}(\rho u_j k) = \frac{\partial}{\partial x_j}\left(\frac{\mu_t}{\sigma_k}\frac{\partial k}{\partial x_i}\right) + G_k + G_b - \rho\varepsilon \tag{8}$$

$$\frac{\partial}{\partial x_j}(\rho u_j \varepsilon) = \frac{\partial}{\partial x_j}\left(\frac{\mu_t}{\sigma_\varepsilon}\frac{\partial \varepsilon}{\partial x_i}\right) + C_1 \frac{k}{\varepsilon}(G_k + G_b)(1 + C_3 R_f) - C_2 \rho \frac{\varepsilon^2}{k} \tag{9}$$

In Eqs. (8) and (9), G_k and G_b are the turbulent production terms of stress and buoyancy force, respectively, and are given by

$$G_k = \mu_t \left(\frac{\partial u_j}{\partial x_i} + \frac{\partial u_i}{\partial x_j} \right) \frac{\partial u_j}{\partial x_i} \tag{10a}$$

$$G_b = -\beta g_i \frac{\mu_t}{\sigma_t} \frac{\partial T}{\partial x_i} \tag{10b}$$

The model constants and various functions used in the $k-\varepsilon$ model are explained in Refs. 7 and 8.

2.3 Numerical optimization

Most of gradient-based optimization technologies are an iterative process in which iterative advancements are performed over successive designs until the optimum values are achieved. The optimization is to find the design variables with the minimized objective function numerically. In this case, the design variables and objective functions are commonly subjected to the constrained conditions. Thus, the nonlinear, unconstrained optimum design problem can be expressed mathematically

$$\text{Find} \quad \boldsymbol{X} = \{X_1, X_2, \cdots, X_N\}^T \tag{11}$$

$$\text{to minimize} \quad F(\boldsymbol{X}) \tag{12}$$

$$\text{subject to} \quad \boldsymbol{X}_i^L \leq \boldsymbol{X}_i \leq \boldsymbol{X}_i^U \quad \text{for } i=1, N \tag{13}$$

where $\boldsymbol{X}$ represents the design variable vector and N is the number of design variables. $F(\boldsymbol{X})$ is the objective function which depends on the values of the design variables. $\boldsymbol{X}_i^L$ and $\boldsymbol{X}_i^U$ are the lower and upper limits of the design variables, respectively, and they simply limit the region of search for the optimization.

The algorithm based on CAO can control only a single objective function and the procedure of optimization is sequentially carried out in the order of the importance of objective functions. Thus, this problem should be reduced to a single-objective optimization problem. Since Koski[9] proposed the typical descriptions of the Pareto technique which is the determination of the compromised set of a multi-objective problem, many mathematical methods for multi-objectives have been developed in the past two decades. Among them, the weighting method has been widely used on the multi-objective problem because the solution can be obtained by choosing the different non-negative weighting coefficients ($\omega_i \geqq 0$). That is, to solve the multi-objective optimization problem by means of the weighting methods, it can be converted into a sequence of scalar optimization problems where the objective function is defined by a linear combination of all the objective functions. In addition, all the objective functions should be expressed in units of approximately the same numerical values. The general form of a multi-objective problem using the weighting method is as follows:

$$\text{Minimize} \quad F(\boldsymbol{X}) = \sum_{i=0}^{o} \omega_i \frac{F_i(\boldsymbol{X})}{F_i^0(\boldsymbol{X})} \tag{14}$$

where ω_i denotes the weighting coefficients representing the relative importance of the each objective function and its sum is unity. $F_i^0(\boldsymbol{X})$ is the objective function corresponding to the baseline geometry.

3. Numerical methodology

Figure 2 shows the numerical methodology for optimization. In order to obtain the optimal values of the heat sink with pin-fins, the three

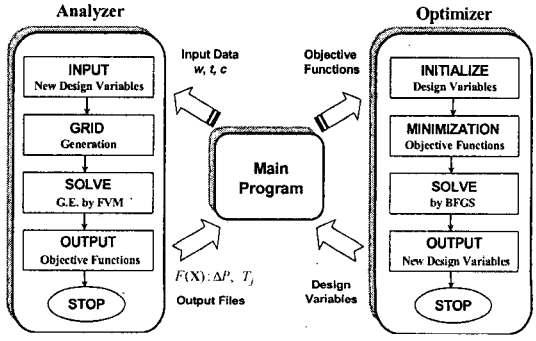

Fig. 2 Optimization procedure.

programs are used; (1) the main program which defines various arrays and parameters, and controls the analyzer and optimizer, (2) the analyzer that evaluates the objective functions and (3) the optimizer which can solve a nonlinear optimization problem.

As mentioned earlier, all of the commercial CFD codes basically solve the flow and thermal characteristics on the GUI. Thus, it is an important task to combine commercial CFD solver with mathematical a optimization method to carry out the optimization automatically. Therefore, the script-file is developed to integrate the different programs and used it for obtaining the otimal solutions, as shown in Fig. 2. Once the objective functions (ΔP and θ_j) are obtained as the results of calculation of flow and thermal fields by the analyzer, the main program calls the optimizer to proceed with optimization. The optimizer may modify the design variables. When the optimizer requires new values of the objective functions, it returns to the main program and the analyzer is called to calculate them. In this step, the analyzer should generate a new grid system because new design variables are proposed by the optimizer. This process is repeated until the optimization is complete and is performed automatically. As a result of optimization, the optimal design variables and the corresponding pressure drop and thermal resistance are obtained.

3.1 Flow and thermal fields

The governing equations for three dimensional turbulent convective heat transfer and fluid flow are solved using FLUENT which is a commercial finite volume CFD code.[10] The reason for using the CFD code is as follows: to obtain the optimum solutions by means of the mathematical optimization technique, a fast and reliable computer program must be used because it operates repeatedly for many different geometrical configurations during the optimization process. The SIMPLE algorithm[11] is used to calculate the pressure correction equation in the momentum equation. The power law scheme is employed for the treatment of convection and diffusion terms.

3.1.1 Boundary conditions

To capture the reverse flow at the exit of the heat sink, we extend the computational domain to five times the heat sink dimension in x- and y-directions from the symmetric surfaces. Figure 3 shows the extended computational domain including the heat sink. A no-slip boundary condition for all solid walls is assigned for velocity. At the inlet of the heat sink, the coolant of a constant temperature (T_{in}=313 K) flows downward with a constant velocity ($w=-4$ m/s) and a swirl condition of 60 rad/s. The corresponding turbulent kinetic energy and its dissipation rate are $k=0.01w_{in}^2$ and $\varepsilon=C_\mu^{4/3}k^{3/2}/l$, here l is a length scale for dissipation, taken here as the length of fan. Uniform heat flux is applied to the heat sink at the center of the bottom wall (12×12 mm) by a heat source (Q=40 W) and the convective boundary condition for temperature is used at the bottom wall except for the heat source. The symmetric conditions are imposed for all dependent variables at the two planes of symmetry (i.e., $x=0$, $y=0$). The pressure boundary condi-

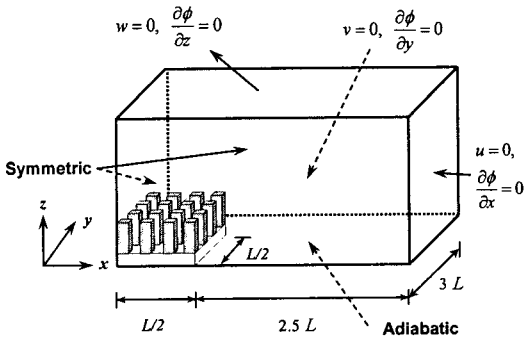

Fig. 3 Boundary conditions for extended computational domain.

tion for velocities is used at all exit planes (that is, $x=3L$, $y=3L$, $z=H+c$) because the boundaries are sufficiently far from the heat sink.

When the sum of residual and the relative error of consecutive iteration for dependent variables are less than 10^{-5}, the solutions are treated as converged ones.

3.2 Unconstrained optimization problem

To minimize the objective function, its gradient is calculated using the finite difference method (FDM) and the design variables are updated by the following equation

$$X_{k+1} = X_k + \alpha_k \cdot S_k \tag{15}$$

where the subscript k is the number of iterations. In Eq. (15), the search direction, S_k, and the step length parameter, α_k, which minimizes the objective function, should be determined in order to complete the optimization process. In this study, to obtain the search direction, we used the BFGS (Broydon-Fletcher-Goldfarb-Shanno) method, which is generally considered to be the most effective method among the variable metric methods, for the unconstrained optimization problem. This method is a kind of quasi-Newton method and has an important merit of a self-correcting mechanism.[12] The BFGS method creates an approximation to the inverse of the Hessian matrix, H (i.e., matrix of second derivatives of the objective function) and enables to define the line search direction for a given iteration by

$$S_{k+1} = -[H_k]^{-1} \cdot \nabla F(X_k) \tag{16}$$

The Hessian approximation H_k is updated at each iteration by means of the following equation:

$$H_{k+1} = \left(H - \frac{H\delta\delta^T H}{\delta^T H \delta} + \frac{\gamma\gamma^T}{\delta^T \gamma} \right)_k \tag{17}$$

where the change vectors, δ_k and γ_k, are given by

$$\delta_k = X_{k+1} - X_k \tag{18a}$$

$$\gamma_k = \nabla F(X_{k+1}) - \nabla F(X_k) \tag{18b}$$

In particular, H satisfies the quasi-Newton condition ($H_{k+1}\delta_k = \gamma_k$) and if $\delta_k^T \cdot \gamma_k > 0$, the H is retained at a positive definiteness. Therefore, the initial Hessian is symmetric and is given a positive definite. The scalar α_k is adopted when the following equations are satisfied

$$\begin{aligned} &F(X_{k+1}) - F(X_k) \le \sigma_1 \nabla F^T(X_k)\delta_k \\ &\text{or} \quad \nabla F^T(X_{k+1})\delta_k \ge -\sigma_2 \nabla F^T(X_k)\delta_k \end{aligned} \tag{19}$$

where $0 \le \sigma_1 \le 0.5$ and $\sigma_1 \le \sigma_2 \le 1.0$.

When the difference between the successive values of the objective function, $F(X)$, satisfies the following convergence criterion, the optimization process terminates:

$$|F(X_{k+1}) - F(X_k)| \le 10^{-5} \tag{20}$$

4. Results and discussion

In this study, the optimization of a pin-fins heat sink is conducted numerically. For a fixed volume of heat sink, a high thermal performance (or cooling efficiency) can be acquired when the thermal resistance and the pressure drop are minimized, simultaneously. Therefore, in this study the objective functions to be minimized are the pressure drop (ΔP) and the junction-to-ambient thermal resistance (θ_j) and they are given by

$$\Delta P = P - P_\infty, \quad \theta_j = \frac{T_j - T_\infty}{Q} \tag{21}$$

where Q is the heat generated through the heat

sink and the subscripts, j and ∞ mean the junction and ambient, respectively, and they are represented as $F_1(X)$ and $F_2(X)$, respectively.

The geometric parameters which strongly influence the thermal performance of the heat sink are the width of fin (w), fin length (h), and fan-to-heat sink distance (c). Thus, we choose them as the design variables.

The mathematical expression for the heat sink optimization can be written as

$$\text{Find} \quad X = [w, h, c] \tag{22}$$

$$\text{to minimize} \quad F(X) = [\Delta P, \theta_j] \tag{23}$$

$$\text{subject to} \quad \begin{aligned} & X_i^L \leqq X_i \leqq X_i^U \\ & 1.0 \leqq w \leqq 9.0 \\ & 32.5 \leqq h \leqq 60.0 \\ & 1.0 \leqq c \leqq 13.0 \end{aligned} \tag{24}$$

The baseline (or initial) geometric parameters considered for optimization are as follows: the fins have a 3 mm width, 45 mm height and a 3 mm of fan-to-heat sink distance. That is, $X_o = [w, h, c; 3.0, 45.0, 3.0]$.

4.1 Parametric studies

The parametric studies are generally performed in order to

(1) investigate the most important design variable in the heat sink performance and

(2) choose the most appropriate optimization algorithm.

For the parametric studies, the degree of importance of each design variable such as the fin width, fin height, and fan-to-heat sink distance is investigated before the design optimization is carried out. That is, the effect of each design variable on the pressure drop and the thermal resistance is examined by varying only one variable among the baseline parameters.

The junction temperature and pressure drop for various fin widths (w) are shown in Fig. 4. In this figure, the other design variables are fixed as the baseline model (i.e., h=45 mm and c=3.0 mm). The figure shows that as the fin width increases, the junction temperature decreases while the pressure drop increases. This phenomena result from the following reasons; for a fixed volume of heat sink ($L = W$=constant), increasing in the fin width enlarges the heat transfer area and results in more heat removal at the solid-air interface, while it causes the pressure drop to increase because the increased fin width plays the role as a blockage of flow passages. From these results, it is easily found that the optimum value of w can be ranged as $3 < w < 5$ mm, which will also be found in Table 1.

Figure 5 presents the effect of the fin height

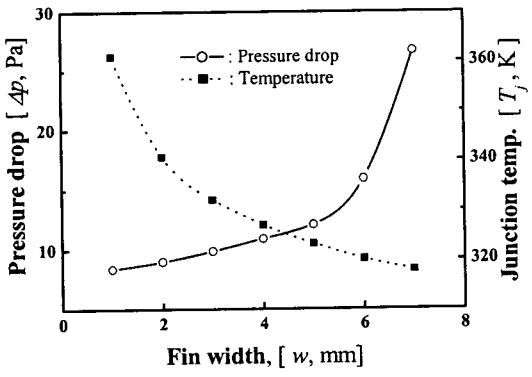

Fig. 4 Effect of fin width (w) at h=45 and c =3 mm.

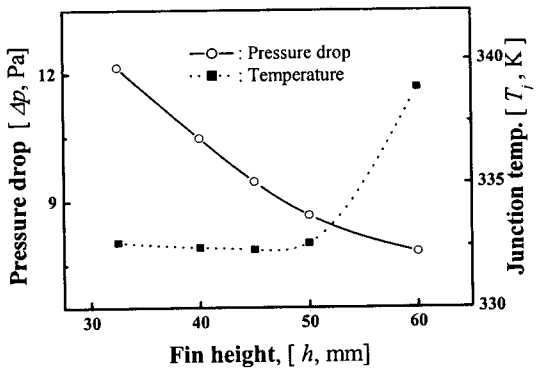

Fig. 5 Effect of fin height (h) at w=3 and c =3 mm.

(h) on the flow and thermal characteristics in the heat sink. As can be seen in Fig. 5, T_j decreases slightly until h=45 mm at which it has a minimum value, and then increases sharply, while the pressure drop reduces linearly as the fin height increases. This is mainly due to the fact that the complex flow characteristics such as vortex and reverse flows occur because more air strikes the heat sink basement as the fin height decrease. From these results, it is easily predicted that the optimum value of h for all weighting coefficients can be ranged between h =50 and 60 mm.

The effect of the fan-to heat sink distance on the junction temperature and pressure drop is also investigated and the results are shown in Fig. 6. Figure 6 shows an interesting phenomenon that as the fan-to-heat sink distance increases, the pressure drop reduces almost linearly. This is due to the fact that a part of the total air flow rate induced by the fan flows towards the outside of the heat sink which has a relatively low pressure than the inside as c increases. The decreased pressure drop results in the increase of junction temperature due to a smaller flow rate. It is also found that the effect of c on the pressure and temperature fields is very small compared to other variables (i.e., variations of pressure drop and junction temperature for the range of c=1 to 15 mm are 2.7 Pa and 2.1 K, respectively).

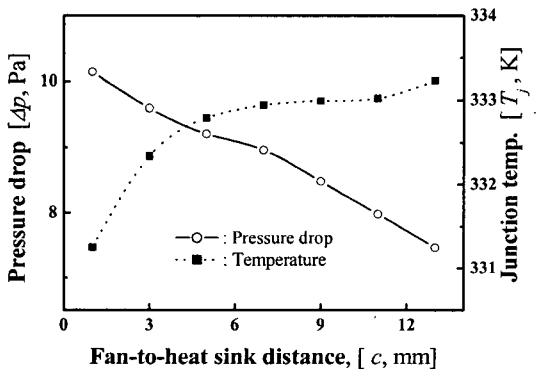

Fig. 6 Effect of fan-to-heat sink distance (c) at w=3 and h=45 mm.

The parametric studies discussed above show that the fin width has a strong influence on the pressure drop and junction temperature in the heat sink, while the effect of fan-to-heat sink distance is relatively small compared to the other two design variables. It can be also found in Figs. 4~6 that the objective function has only one minimum value (see the junction temperature in Fig. 5) or simply increases or decreases within the range of design variables. The existence of an unique minimum value for the objective functions indicates that the local optimization technique such as the BFGS method becomes an effective optimization algorithm rather than the global optimization.

4.2 Optimal solutions

The optimum design variables can be obtained by minimizing both the thermal resistance and pressure drop in the heat sink. Therefore, the results for the multi-objective function problem are obtained by using the following normalized equation in which the weighting coefficient (ω_i) is used,

$$F(X) = \omega_1 \cdot \left(\frac{F_1(X)}{\Delta P^0} \right) + \omega_2 \cdot \left(\frac{F_2(X)}{\theta_j^0} \right) \quad (25)$$

where the superscript o depicts the initial condition. In this study, the initial thermal resistance (θ_j^0) with a junction temperature of 349.8 K is 0.92 K/W and the initial pressure drop (ΔP^0) is calculated as 9.68 Pa. Note that an increase in the weighting coefficient of ω_1 means that the minimized pressure drop is more important than the minimized thermal resistance.

Figure 7 shows the convergence history for the pressure drop (i.e., one of the objective functions) during optimization for the cases of ω_1=0.7 and ω_2=0.3. Initially, there is a sharp

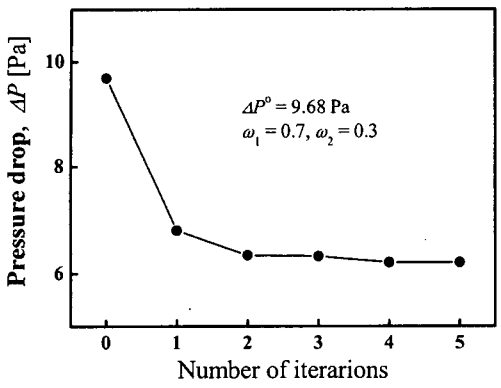

Fig. 7 Convergence history of the pressure drop for $\omega_1=0.7$ and $\omega_2=0.3$.

decrease in the pressure drop and it is converged after about five iterations. This figure also shows that ΔP is reduced by 35.85% from the initial value of 9.68 Pa to an optimum value of 6.21. However, it is true that the number of iterations for convergence is usually changed according to the weighting coefficients used.

Table 1 and 2 present the optimum design variables and the corresponding objective functions for various weighting coefficients, respectively. We are also able to compare each optimum solution from this table because it shows the results of the degree of importance of the two objective functions. In particular, the design variables can be obtained directly from Table 2 for the most useful geometrical configurations of the pin-fins heat sink. As we expected, the optimum design variables are varied along the weighting coefficient. For example, as ω_1 is increased from 0.1 to 0.9, the pressure drop is reduced by 25.4% from 8.10 to 6.05 Pa. However, these values are decreased by 16.3 and 37.6%, respectively, compared to the baseline condition. On the contrary, the thermal resistance is increased from 0.518 to 0.752 K/W for $\omega_1=0.1$ and $\omega_2=0.9$. This clearly shows that for the design of the heat sink with pin-fins, it is very important to choose the proper design variables by considering which one is preferable between the pressure drop and the thermal resistance. It can be easily found from Table 1 that the fin width (w) is reduced as the pressure drop decreases because the in crease of ω_1 is intended to decrease the pressure drop. That is, the optimizer tries to find the design values for reducing the pressure drop during the optimization process. Table 1 also shows an interesting result that for $\omega_1>0.7$, the fin height (h) does not change and approaches its upper constraint value of 60 mm. This means that the fin thickness has little effect on reducing the pressure drop when the weighting coefficient for pressure drop is greater than 0.7.

Table 1 Optimum design values for the change of weighting coefficients [mm]

ω_1	ω_2	w	h	c
0.1	0.9	4.85	57.8	2.41
0.3	0.7	4.72	58.4	2.47
0.5	0.5	4.65	59.2	2.67
0.7	0.3	4.59	60.0	2.72
0.9	0.1	4.31	60.0	2.77

Table 2 Thermal resistance and pressure drop for optimal and baseline models for various weighting coefficients

Optimum model		θ_j [K/W]	ΔP [Pa]
ω_1	ω_2		
0.1	0.9	0.518	8.10
0.3	0.7	0.543	7.56
0.5	0.5	0.568	6.91
0.7	0.3	0.687	6.21
0.9	0.1	0.752	6.05
Baseline model		0.92	9.68

A set of optimal solutions for the objective functions can be constructed and it can help the designer to select the preferred solutions based on Table 1. For this purpose, the relationship between the objective functions (ΔP and θ_j) is illustrated in Fig. 8. The solutions along the curve from (a) to (e) are called as the set of Pareto optimal solutions. The results

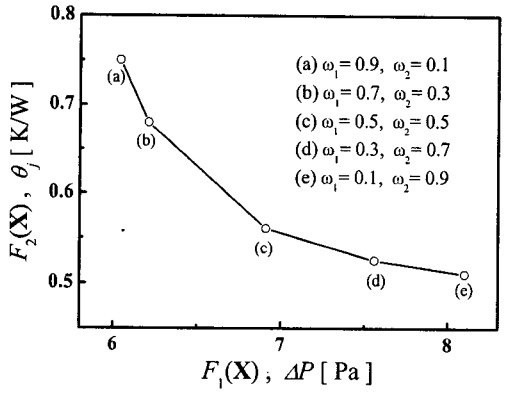

Fig. 8 Pareto solutions for heat sink.

can be very helpful to designers for achieving the optimal values of heat sink. For example, when designers want to focus on decreasing the thermal resistance rather than decreasing the pressure drop, they can select the points such as (c), (d), and (e) on the curve of Fig. 8 and then read the corresponding optimal values of the design variables in Table 1. For the thermal management of the heat sink, it is important to remark that the fundamental goal of heat sink design is to minimize the thermal resistance (i.e., maximize the heat transfer rate) and this is easily achieved by the increases of velocity between fins and heat transfer area. Unfortunately, however, an increase in velocity results in increasing the pressure loss. The minimized pressure drop is strongly related to the specific cost, because the pressure drop determines the size of the fan needed to blow the cool air through the channel. Therefore, choosing one of the Pareto solutions is dependent on the heat sink designers.

5. Conclusions

We numerically investigated the optimum design variables of a 7×7 pin-fins heat sink to minimize the thermal resistance between the chip and heat sink, and the pressure drop in the heat sink. The most dominant design variables for the pressure drop and thermal resistance were the fin width (w), and the fin height (h), while the effect of fan-to-heat sink distance on them was relatively small.

The local optimization technique, which was used in this study, was more effective than the global scheme. The results also showed that the optimal values of the design variables for the weighting coefficient of 0.5 were w= 4.65 mm, h=59.22 mm, and c=2.67 mm. Additionally, the thermal resistance for the optimum model was decreased by 37.7% and the pressure drop was also decreased by 28.5% compared to those of the baseline model. The optimization could be completed as the graph of Pareto optimal solutions was plotted for two objective functions. The results of this work offer designers the information they need to select the optimal design variables corresponding to the preferred objective functions.

Acknowledgement

This research was supported by The Center of Innovative Design Optimization Technology (iDOT), Korea Science and Engineering Foundation.

References

1. Gallman, J. W., Smith, S. C. and Kroo, I. M., 1993, Optimization of joined-wing aircraft, J. of Aircraft, Vol. 30, No. 6, pp. 897-905.
2. Craig, K. J., Venter, P. V., de Kock, D. J. and Suyman, J. A., 1999, Optimisation of structured grid spacing parameters for separated flow simulation using mathematical optimization, J. of Wind Enginering and Industrial Aero- dynamics, Vol. 80, pp. 221-231.
3. Park, K., Choi, D. H. and Lee, K. S., 2003, Design optimization of plate-fin and tube heat exchanger, Numerical Heat Transfer Part A, Vol. 45, pp. 347-361.
4. Ledezma, G., Morega, A. M. and Bejan, A., 1996, Optimal spacing between pin fins with

impinging flow, ASME J. of Heat Transfer, Vol. 118, pp. 570-577.
5. Maveety, J. G. and Hendricks, J. F., 1999, A heat sink performance study considering material, geometry, nozzle placement, and Reynolds number with air impingement, ASME J. of Electronic Packaging, Vol. 121, pp. 156-161.
6. Maveety, J. G. and Jung, H. H., 2000, Design of an optimal pin-fin heat sink with air impingement cooling, Int. Comm. Haet Mass Transfer, Vol. 27, pp. 229-240.
7. Rodi, W., 1984, Turbulence models and their applications in hydraulics a state-art-of review, Book Publication of International Association for Hydraulic Research, Delft, Netherlands.
8. Abe, K., Kondoh, T. and Nagano, Y., 1996, A two-equation heat transfer model reflecting second-moment closures for wall and free turbulent flows, Int. J. Heat and Fluid Flow, Vol. 17, pp. 228-237.
9. Koski, J., 1984, Multicreterion optimization in structural design, in New directions in optimum structural design, John Wiley, New York, pp. 483-503.
10. FLUENT 6 User's Guide, FLUENT Inc., 2003.
11. Patankar, S. V., 1980, Numerical heat transfer and fluid flow, Hemisphere, Washington.
12. Nocedal, J., 1992, Theory of algorithms for unconstrained optimization, Acta Numerica, Vol. 1, pp. 199-242.